

Supplementary Information: Energy and Temperature Dependence of Rigid Unity Modes within AlPO_4

Adam Berlie, Gordon J. Kearley, Yun Liu, Dehong Yu, Richard A. Mole, Chris D. Ling and R. L. Withers

Analysis of Quasi-Elastic Neutron scattering

Within this section we will briefly detail the analysis of the QENS data within the manuscript. QENS was only observed within the spectrum obtained at 300 K and at 100 K the dynamic behaviour had likely moved to a time scale outside of the experiment. All data was analysed within the LAMP program [1] which enabled manipulation of the raw data and analysis of the QENS as a function of Q using STRfit. It should be noted that this experiment was set up primarily to conduct inelastic measurements and so the QENS data collection was not fully optimised for this experiment.

From the raw data the detectors that showed a Bragg peak were removed from the spectrum which should leave only the elastic and inelastic incoherent scattering as shown in figure S1.

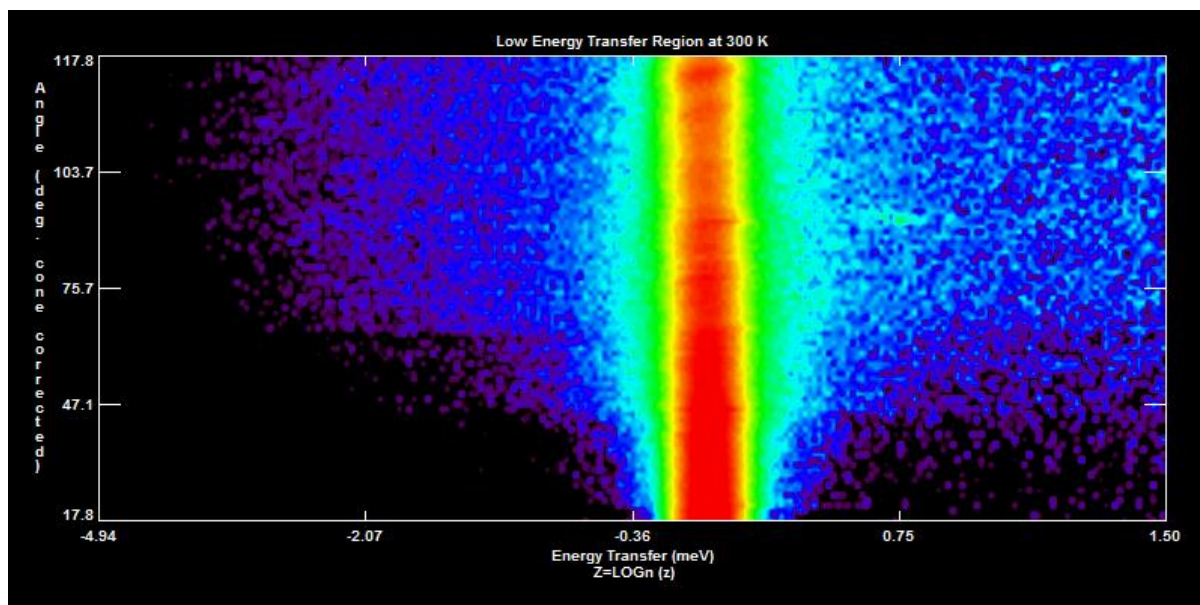


Figure S1: Spectrum of AlPO_4 after the subtraction of detectors where a Bragg peak was present. The scale (in the z -direction or coming out of the page) follows the colours of the rainbow and black/purple is the lowest intensity and red is the highest. Note that the y -axis is in detector angle (in units of 2θ), however elastic $Q = 4\pi\left(\frac{\sin(\theta)}{\lambda}\right)$ where θ is the angle and λ is the wavelength. Therefore increasing angle corresponds to increasing Q .

From figure S1 one can see that as Q increases the contribution of the QENS increases, although we are limited by our energy range due to kinematic consequences. This is as expected as the diffusive motion become more dominant as the length scale decreases or as you go out in reciprocal space.

To fit the data STRfit was used which accounts for the instrumental broadening of the elastic peak. A vanadium scan was obtained at 300 K and this was used to calculate the instrumental resolution within the program itself and deconvolute the raw data. It was then found that the best model to fit the data was

$$QENS = \delta(Q) + L_1(Q) + L_2(Q)$$

where $\delta(Q)$ is a delta function that accounts for the elastic peak and $L_n(Q)$ is a Lorentzian relaxation which is a feature of the QENS.

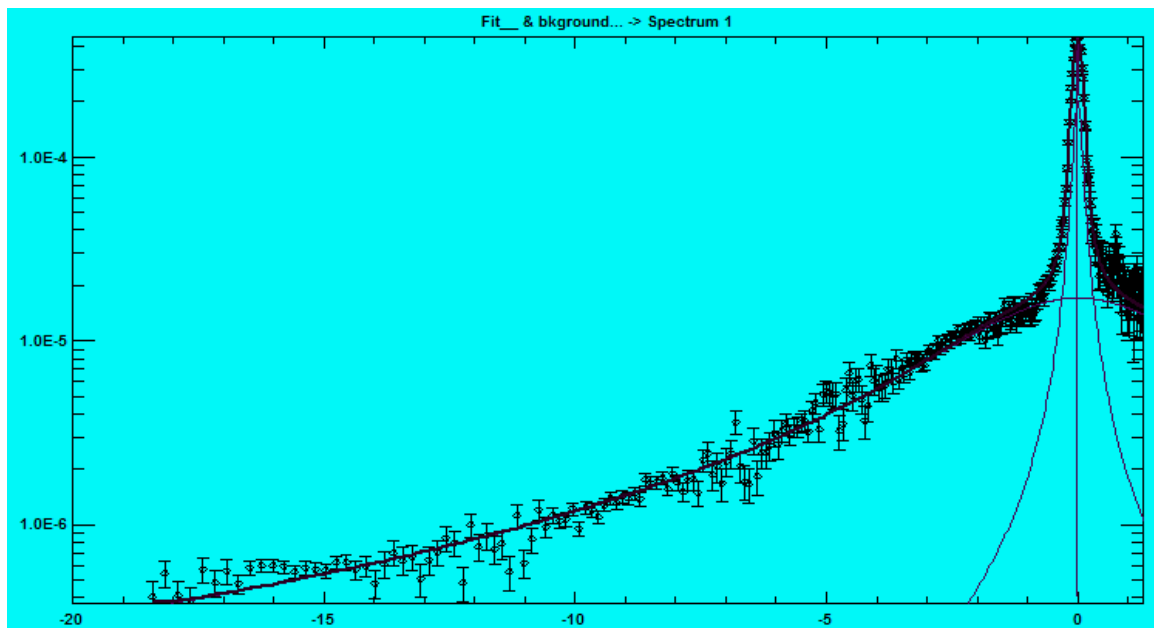


Figure S2: Fit to the QENS behaviour at $Q = 2 \text{ \AA}^{-1}$ where the two Lorentzians likely correspond to two different relaxation processes. Note that the ordinate corresponds to the intensity and the abscissa corresponds to energy transfer (meV).

At $Q = 2 \text{ \AA}^{-1}$ the fit to the QENS data can be seen in figure S2 where the two Lorentzians used account for two different relaxation processes present within the sample. For $Q = 2 \text{ \AA}^{-1}$, $\lambda_1 = 5.46 \text{ meV}^{-1}$ and $\lambda_2 = 0.19 \text{ meV}^{-1}$, which equates to

average relaxation time scales of approximately 0.5 ps and 10 ps respectively, thus the two processes are occurring on very different time scales.

The data was fit over the entire Q range that was accessible within the experiment and two relaxation parameters can be seen in figure S3. As mentioned the data has two distinct relaxations that occur on different timescales. The

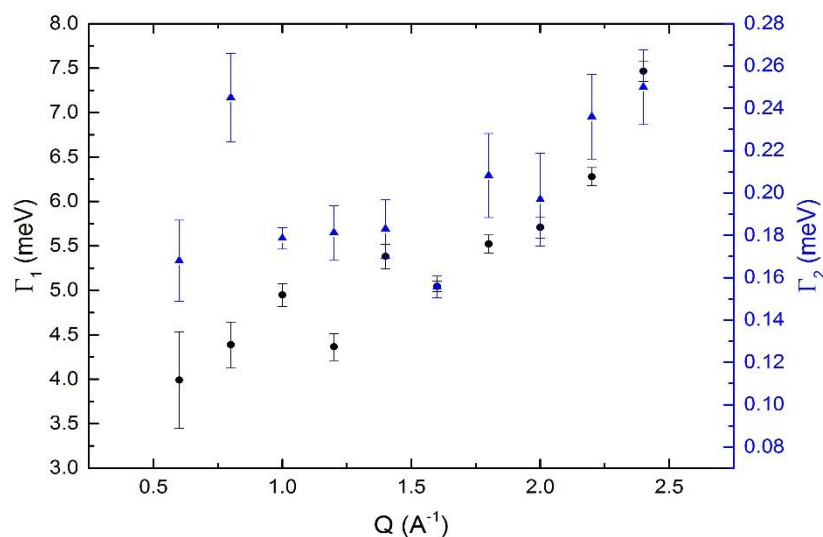


Figure S3: Lorentzian relaxation parameters from fits to the QENS data over the accessible Q range. Two different relaxations were observed, one that accounts for both the fast and slow relaxation.

width of the peak is what give information on the time scale of the diffusive motion and the 1st relaxation is much faster than the 2nd.

The Elastic Incoherent Structure Factor (EISF) provides a measure of what the QENS component is doing as a function of Q as it can show the probability of finding the particle at R_0 after infinite time if it was at R_0 at time = 0. If time is infinite, this is considered the resolution of the instrument and at $Q = 0$ this is related to the inverse of the volume where the particle is considered to be present. Therefore at $Q = 0$ the particle must always be present and so the EISF must always equal 1. Overall this method can provide information on the length scale of the diffusive motion. Figure S4 shows the combined EISF for the two components where there is a clear dip at approximately 1.6 \AA^{-1} and in the case the EISF is defined as

$$EISF = \frac{A_\delta}{(A_\delta + A_{\lambda 1} + A_{\lambda 2})}$$

where A_n accounts for the amplitude of the delta function, 1st and 2nd Lorentzians respectively. The red line shows a calculation based on a spherical diffusion model with a radius of $Q = 1.6 \text{ \AA}^{-1}$ or $r = 1.8 \text{ \AA}$. Although this is an approximation there is a good match between the observed and simulated data sets. If one separates out the 2 components and plots the EISF, the data still shows a dip at approximately 1.6 \AA^{-1} and so both processes occur over a similar length scale. Note

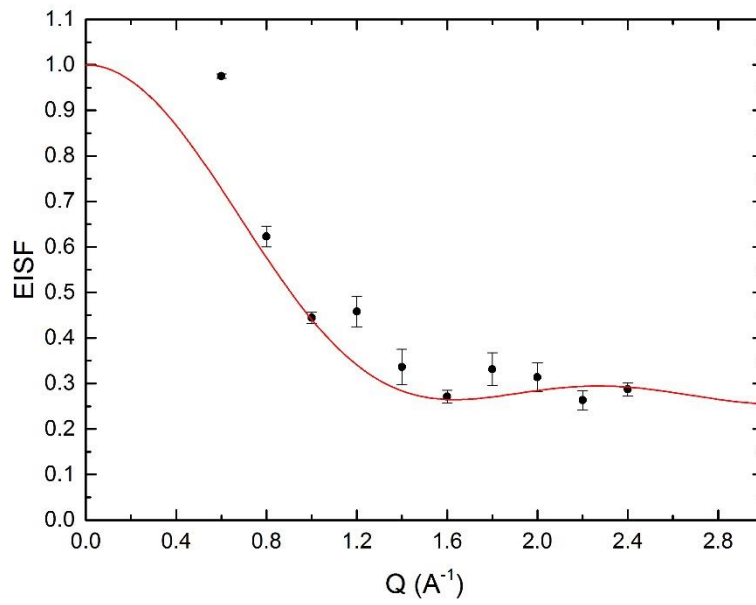


Figure S4: Total EISF for both components as a function of Q . The red line is a calculation based on a spherical diffusion model with a radius of 1.8 \AA .

that a baseline of 0.2 was present within the EISF and this may be due to the fact that there is some coherent scattering present that has not been subtracted from the data.

Although the quality of the data is limited, since, as mentioned, this experiment was primarily set up to look at the inelastic scattering, there is a clear trend and we have been able to get an approximate length scale for the diffusive process of both components. In order to attempt to assign this diffusive motion to a particular process one must first consider an MO_4 ($M = Al$ or P) tetrahedron where $Al-O = 1.76 \text{ \AA}$ and $P-O = 1.54 \text{ \AA}$. On average the $M-O$ bond length would be 1.66 \AA and this is well within the regime of the dip seen within the Q dependence of the EISF. Therefore this diffusive motion may be the tetrahedron rocking around the sphere, it should be noted that due to confinement by other bonded

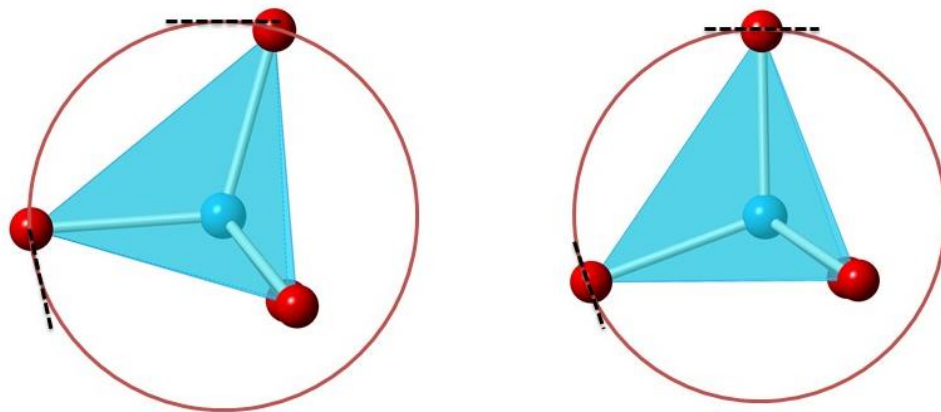


Figure S5: AlO_4 tetrahedra superimposed onto a circular or spherical model where in this case the $Al-O$ bond length is 1.76 \AA (note $P-O = 1.54 \text{ \AA}$).

tetrahedra outside this sphere it is not unrestricted motion across the sphere. Instead the rocking motion is confined to areas marked by the black dotted lines. It should be noted that our model of the QENS is supported by MD calculations performed and crystallographic data so the description may not be far from what we propose.

Ultimately more analysis and experimental evidence is needed but there are clearly two different components and so more work is needed to unravel this and create a good model to describe the data/system. Additional experiments to solve this will be conducted in the future.

Heat Capacity

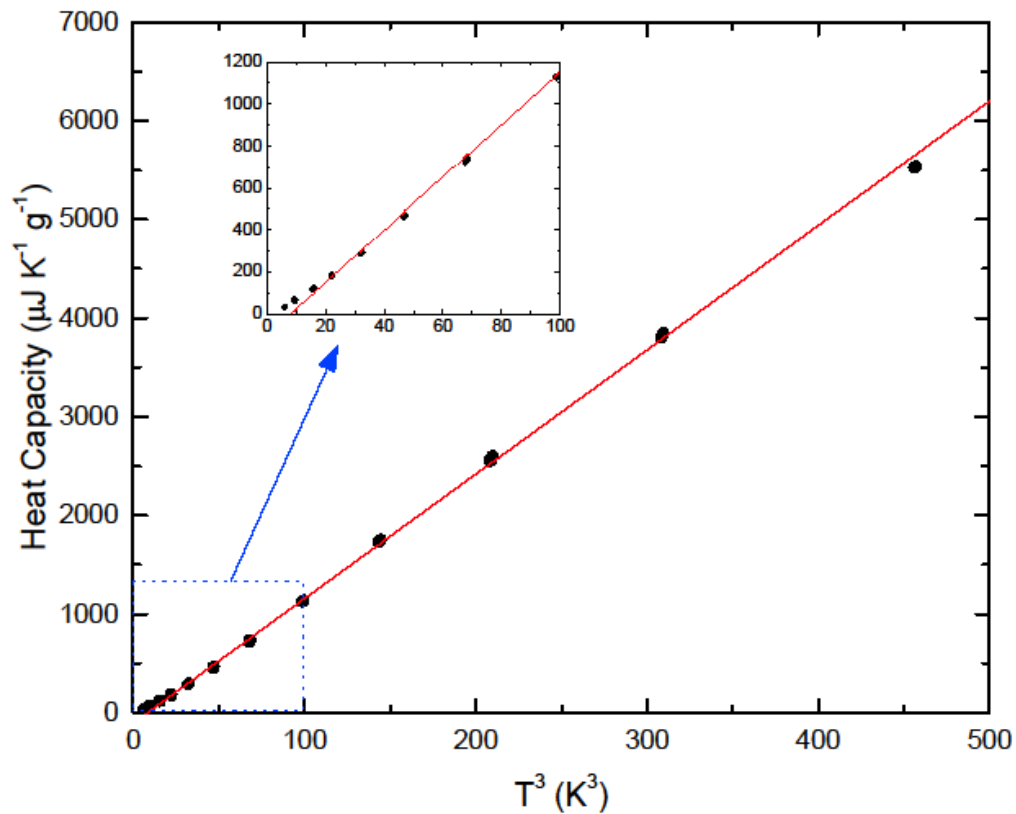


Figure S6: Low temperature fit to the AlPO₄ heat capacity data using Equation 1 from the paper. At very low temperatures there is a deviation from the linear T³ behaviour suggesting that the structural disorder is increasing.

References:

1. D. Richard, M. [Ferrand](#) and G.J. [Kearley](#). *J. Neutron Research*. **4** (1996) 33